Journal of Sound and Vibration (1997) **208**(2), 271–287

PARAMETER IDENTIFICATION FOR ALUMINUM HONEYCOMB SANDWICH PANELS BASED ON ORTHOTROPIC TIMOSHENKO BEAM THEORY

T. SAITO

Faculty of Engineering, Yamaguchi University, 2557 Tokiwadai, Ube, Yamaguchi 755, Japan

R. D. PARBERY

Department of Mechanical Engineering, The University of Newcastle, University Drive, Callaghan, NSW 2308, Australia

S. OKUNO

Mechanical Laboratory, Hitachi Company Ltd, 794 Higashitoyoi, Kudamatsu, Yamaguchi 744, Japan

AND

S. KAWANO

Faculty of Engineering, Yamaguchi University, 2557 Tokiwadai, Ube, Yamaguchi 755, Japan

(*Received* 13 *January* 1997, *and in final form* 6 *June* 1997)

The present paper deals with parameter identification of aluminum honeycomb sandwich panels with the assumption that they can be treated as orthotropic continua. Elastic constants and modal damping ratios are considered as the identified parameters, and the basic equations of Timoshenko beam theory are employed in this paper. The numerical identification problem of minimizing the errors between the experimental and the analytical results leads to two optimization problems. We introduce, as objective functions, an error function calculated by the natural frequencies and another by the accelerances. Both non-linear optimization problems with constraints are solved by the downhill simplex method including a penalty function. The density is obtained experimentally and in the first optimization problem only the elastic constants are identified. For the second optimization problem, both elastic constants and modal damping ratios are identified simultaneously. The resulting parameters are applied to finite element analysis and the calculated time histories of accelerations are compared with the experimental results to examine the validity of these identified parameters.

1. INTRODUCTION

Aluminum honeycomb sandwich panels have such superior characteristics in bending stiffness and in spite of the light weight that they are used in many engineering applications, such as automobiles, railways or aerospace vehicles. The Japanese Railway Company is likely to consider their application for the vehicles of the next superexpress. To date, various papers concerned with the characteristics of honeycomb sandwich panels have been published [1–11]. Most of them have treated the buckling problems from the angle of material strength by analysis of honeycomb cores [1–7]. However, although serious vibration and noise problems can be anticipated to occur in such high speed vehicles as aeroplanes or superexpress trains, several important vibration problems are still left

0022–460X/97/470271 + 17 $25.00/0/sv971189

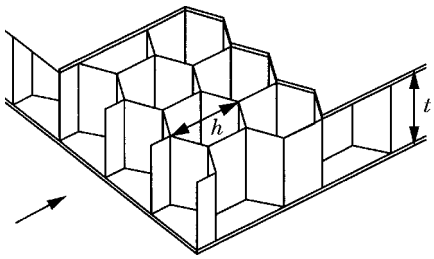

Figure 1. The honeycomb sandwich panel.

unsettled [8–10]. This omission originates in the difficulty of applying a general material test to these materials [11], since they do not always have isotropic structure and have the characteristics of high bending rigidity but small shear rigidity in the direction of the thickness. Available information about such properties as elastic constants and damping coefficients is insufficient to investigate the dynamic response. Recently, engineers using the finite element method (FEM) in their design or analysis have succeeded in obtaining results for the dynamic characteristics. After selecting a proper finite element model, they have to determine the material parameters, such as elastic constants, damping ratios and so on, corresponding to the model. We need to develop adequate models of the material and determine their parameters, so as to predict the dynamic response in particular engineering applications of the new materials.

In this paper, we treat the flexural vibration of aluminum honeycomb sandwich panels and identify the parameters. They are not isotropic and have regular but locally different structures. However, we assume that they are orthotropic continuum bodies. The required parameters for continuum bodies, elastic constants and modal damping ratios are identified by analytical and experimental results simultaneously. In this paper, we treat an aluminum honeycomb sandwich panel as an orthotropic Timoshenko beam and identify the corresponding parameters by solving the least squares problems by a non-linear optimization method, the downhill simplex method.

2. MATHEMATICAL MODEL

2.1. AN ALUMINUM HONEYCOMB SANDWICH PANEL

Generally, a honeycomb sandwich panel consists of hexagonal aluminum honeycomb cores and two thin plates. In the panels used in this research, the plates are also aluminum. A schematic view of an aluminum honeycomb sandwich panel is shown in Figure 1. The aluminum honeycomb sandwich panels treated in this paper have two thicknesses, 0·03 m and 0·06 m, and the dimensions of the constituent panels are shown in Table 1. One could analyze it more exactly by considering the dynamics of each sandwich plate and each

TABLE 1

Constitution of sandwich panel

	Panel (1)	Panel (2)
Thickness of panel, t (m)	0·03	0·06
Thickness of sandwich plate (m)	$1{\cdot}0 \times 10^{-3}$	$0{\cdot}75 \times 10^{-3}$
Thickness of hexagonal cell (m)	$0{\cdot}2 \times 10^{-3}$	$0{\cdot}2 \times 10^{-3}$
Dimension h (m)	$2{\cdot}25 \times 10^{-2}$	$3{\cdot}45 \times 10^{-2}$

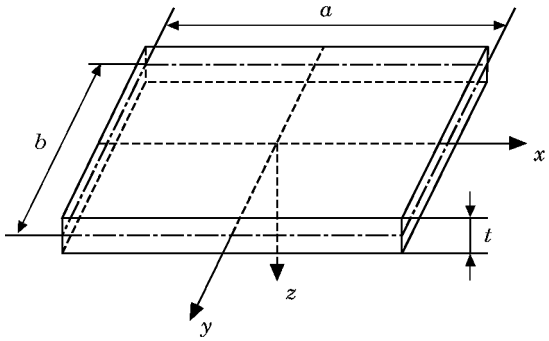

Figure 2. The co-ordinate system.

aluminum honeycomb core simultaneously. However, for simplicity, we treat this sandwich panel as a continuum body when considering flexural vibration globally. As shown in Figure 1, the core rows in the direction of the arrow are different from those in the perpendicular direction. Therefore, we assume that the in-plane properties must be different in the direction of the arrow in Figure 1 and in the normal direction. The out-of-plane properties may well be different from the in-plane properties. Therefore, we regard the aluminum honeycomb sandwich panel as an orthotropic material and introduce a corresponding mathematical model.

2.2. STRESS–STRAIN RELATION

When we treat the mathematical model for flexural vibration of honeycomb sandwich panels, we can take the co-ordinate system as shown in Figure 2. Putting the centre of gravity at the origin, we take the inner plane as the xy–plane and the flexural direction as the z-axis. Then we assume that both the directions of x and y coincide with each principal axis of the material and assign the x direction to that of the arrow shown in Figure 1. The panel has a thickness of t and the dimensions $a \times b$. A plane stress state is assumed in plate or beam theory. Therefore, putting the stress and strain vector as follows

$$\boldsymbol{\sigma} = \{\sigma_x \quad \sigma_y \quad \tau_{xy} \quad \tau_{yz} \quad \tau_{zx}\}^{\mathrm{T}},$$

$$\boldsymbol{\varepsilon} = \{\varepsilon_x \quad \varepsilon_y \quad \gamma_{xy} \quad \gamma_{yz} \quad \gamma_{zx}\}^{\mathrm{T}},$$

we can express the stress–strain relation in an orthotropic plate as follows:

$$\boldsymbol{\sigma} = \mathbf{E}\boldsymbol{\varepsilon}, \tag{1}$$

where $\mathbf{E}$ is the elasticity matrix for the orthotropic material, and is expressed as follows.

$$\mathbf{E} = \frac{1}{1 - \nu_{xy}\nu_{yx}} \begin{bmatrix} E_x & \nu_{xy}E_y & 0 & 0 & 0 \\ \nu_{yx}E_x & E_y & 0 & 0 & 0 \\ 0 & 0 & G_{xy} & 0 & 0 \\ 0 & 0 & 0 & G_{yz} & 0 \\ 0 & 0 & 0 & 0 & G_{zx} \end{bmatrix}, \tag{2}$$

where $v_{xy}E_y = v_{yx}E_x$. Therefore, in flexural vibration problems of plate theory, the following six elastic constants are essential:

$$E_x, \quad E_y, \quad v_{xy} \text{ (or } v_{yx}), \qquad G_{xy}, \quad G_{yz}, \quad G_{zx}.$$

Some flexural vibrations in engineering can be looked upon as those of beams. In the special case in which the width is narrow compared to the length, we can treat the phenomenon as a one-dimensional problem. Namely, when b is negligible compared to a, we can give the stress–strain relation as follows:

$$\sigma_x = E_x\varepsilon_x, \qquad \tau_{zx} = G_{zx}\gamma_{zx}. \tag{3}$$

Therefore, in this circumstance only two elastic constants, E_x and G_{zx}, are necessary. On the other hand, if a is small compared to b, we can treat the phenomenon as another one-dimensional problem. Then, we can give the stress–strain relation as follows:

$$\sigma_y = E_y\varepsilon_y, \qquad \tau_{yz} = G_{yz}\gamma_{yz}. \tag{4}$$

and we can consider another pair of elastic constants E_y and G_{yz}.

In this paper, we consider a beam model related to equation (3) as a preliminary investigation prior to examining a plate or a shell model.

2.3. THE TIMOSHENKO BEAM MODEL

As a mathematical model, we employ Timoshenko beam theory incuding rotational inertia and shear deformation [12], since shearing deformation is likely to occur due to lower shearing rigidity as compared with high bending rigidity in this material. As shown in Figure 3, we denote the flexural displacement by w and the rotation of the cross-sectional area by ψ. Then the equations of motion for the beam subjected to a concentrated force $f(t)$ at $x = l_1$ are expressed as follows:

$$\frac{\partial}{\partial x}\left(E_xI_z\frac{\partial\psi}{\partial x}\right) - k'G_{zx}A\left(\frac{\partial w}{\partial x} + \psi\right) - \rho I_z\frac{\partial^2\psi}{\partial t^2} = 0,$$

$$\frac{\partial}{\partial x}\left\{k'G_{zx}A\left(\frac{\partial w}{\partial x} + \psi\right)\right\} - \rho A\frac{\partial^2 w}{\partial t^2} + f(t)\delta(x - l_1) = 0, \tag{5}$$

where $A = bt$ is a cross-sectional area and $I_z = bt^3/12$ is a secondary moment of inertia. k' denotes the shear coefficient in the Timoshenko beam determined by the cross-sectional shape, and we use the value 2/3, which Timoshenko calculated for the rectangular section [13]. $\delta(x)$ is the Dirac delta function to express the concentrated force. As we carry out the experiments with free boundary conditions, we can put the boundary conditions at $x = \pm a/2$ as follows:

$$E_xI_z\frac{\partial\psi}{\partial x} = 0, \quad k'G_{zx}A\left(\frac{\partial w}{\partial x} + \psi\right) = 0. \tag{6}$$

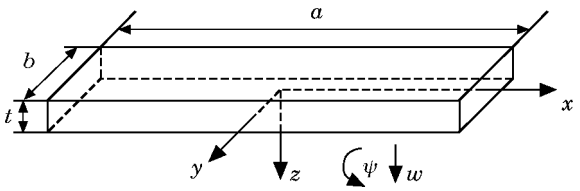

Figure 3. The co-ordinate system for the beam model.

These conditions denote that both the moment and the shear force are zero at both ends of the beam. Then if we consider E_x, I_z, G_{zx} and A as independent of x, and the force $f(t)$ does not act on the beam, we can put general solutions for the mth mode of the normal mode as follows:

$$w = c_1 \, e^{\lambda_m x} \, e^{j\omega_m t} = W_m(x) \, e^{j\omega_m t},$$

$$\psi = c_2 \, e^{\lambda_m x} \, e^{j\omega_m t} = \Psi_m(x) \, e^{j\omega_m t}, \tag{7}$$

where c_1 and c_2 are arbitrary constants, j is the imaginary unit, and λ_m and ω_m are, respectively, the mth characteristic root and the natural angular frequency. $W_m(x)$ and $\Psi_m(x)$ are the mth normal mode function for the motions w and ψ. Substituting equation (7) into equation (5) leads to the characteristic equation for λ_m. When we solve it, we can obtain the characteristic roots as follows:

$$\lambda_m^2 = \frac{1}{2E_x I_z}\left\{-\omega_m^2\left(\rho I_z + \frac{\rho A E_x I_z}{k' G_{zx} A}\right) \pm \sqrt{\omega_m^4\left(\rho I_z - \frac{\rho A E_x I_z}{k' G_{zx} A}\right)^2 + 4E_x I_z \rho A \omega_m^2}\right\}. \tag{8}$$

The above roots depend on an inequality relation between the first and second terms in equation (8); that is, whether or not, the following inequality holds:

$$1 - \frac{\rho I_z}{k' G_{zx} A}\,\omega_m^2 \geqslant 0. \tag{9}$$

When the above inequality holds, the characteristic root λ_m takes two real and two imaginary values, and there are four imaginary values when it does not. When equation (9) is true, the general solutions are expressed as follows:

$$W_m(x) = c_{1m} \cos \alpha_m x + c_{2m} \sin \alpha_m x + c_{3m} \cosh \beta_m x + c_{4m} \sinh \beta_m x,$$

$$\Psi_m(x) = \left(\alpha_m - \frac{\rho A \omega_m^2}{k' G_{zx} A \alpha_m}\right) c_{1m} \sin \alpha_m x - \left(\alpha_m - \frac{\rho A \omega_m^2}{k' G_{zx} A \alpha_m}\right) c_{2m} \cos \alpha_m x$$

$$- \left(\beta_m + \frac{\rho A \omega_m^2}{k' G_{zx} A \beta_m}\right) c_{3m} \sinh \beta_m x - \left(\beta_m + \frac{\rho A \omega_m^2}{k' G_{zx} A \beta_m}\right) c_{4m} \cosh \beta_m x, \tag{10}$$

where the characteristic roots are put as $\lambda_m = \pm j\alpha_m$ and $\pm \beta_m$. Applying the boundary conditions, we can obtain the following frequency equation when the inequality holds in condition (9):

$$\left\{\left(\alpha_m^2 - \frac{\rho A \omega_m^2}{k' G_{zx} A}\right) \cos \frac{\alpha_m l}{2} \, \alpha_m \sinh \frac{\beta_m l}{2} + \left(\beta_m^2 + \frac{\rho A \omega_m^2}{k' G_{zx} A}\right) \cosh \frac{\beta_m l}{2} \, \beta_m \sin \frac{\alpha_m l}{2}\right\}$$

$$\times \left\{\left(\alpha_m^2 - \frac{\rho A \omega_m^2}{k' G_{zx} A}\right) \sin \frac{\alpha_m l}{2} \, \alpha_m \cosh \frac{\beta_m l}{2} - \left(\beta_m^2 + \frac{\rho A \omega_m^2}{k' G_{zx} A}\right) \sinh \frac{\beta_m l}{2} \, \beta_m \cos \frac{\alpha_m l}{2}\right\} = 0. \tag{11}$$

Generally, equations (8) and (11) are functions of characteristics roots λ_m and natural angular frequencies ω_m, and we can use these equations to obtain the natural frequencies

and modes. On the other hand, when we have information about eigenvalue characteristics, we can look upon them as functions of the longitudinal elastic constant E_x and the shear elastic constant G_{zx}.

To calculate the dynamic response, especially the accelerance, we introduce the normal mode approach. We assume that we can express ψ and w respectively in normal mode series as follows:

$$\psi = \sum_{m=-1}^{\infty} \Psi_m(x) a_m(t), \qquad w = \sum_{m=-1}^{\infty} W_m(x) a_m(t), \tag{12}$$

where $m = -1$ and $m = 0$ correspond to the rigid motions of translation and rotation, respectively, with zero frequency and these result from the free boundary conditions. Substituting equation (12) into equation (5), we have the following equations:

$$\sum_{m=-1}^{\infty} \left[\frac{\mathrm{d}}{\mathrm{d}x} \left\{ E_x I_z \frac{\mathrm{d}\Psi_m(x)}{\mathrm{d}x} \right\} a_m(t) - k' G_{zx} A \left\{ \frac{\mathrm{d}W_m(x)}{\mathrm{d}x} + \Psi_m(x) \right\} a_m(t) - \rho I_z \Psi_m(x) \ddot{a}_m(t) \right] = 0,$$

$$\sum_{m=-1}^{\infty} \left[\frac{\mathrm{d}}{\mathrm{d}x} \left\{ k' G_{zx} A \left\{ \frac{\mathrm{d}W_m(x)}{\mathrm{d}x} + \Psi_m(x) \right\} \right) a_m(t) - \rho A W_m(x) \ddot{a}_m(t) \right] + f(x)\delta(x - l_1) = 0,$$

where $(\dot{})$ implies partial differentiation with respect to time. Multiplying these equations by $\Psi_s(x)$ and $W_s(x)$ $(s = -1, 0, \ldots)$ respectively and integrating the products over the length of the beam, we obtain

$$\int_x \sum_{m=-1}^{\infty} \left[\left(\frac{\mathrm{d}}{\mathrm{d}x} \left\{ E_x I_z \frac{\mathrm{d}\Psi_m(x)}{\mathrm{d}x} \right\} \Psi_s(x) - k' G_{zx} A \left\{ \frac{\mathrm{d}W_m(x)}{\mathrm{d}x} + \Psi_m(x) \right\} \Psi_s(x) \right) a_m(t) \right.$$
$$\left. - \rho I_z \Psi_m(x) \Psi_s(x) \ddot{a}_m(t) \right] \mathrm{d}x = 0,$$

$$\int_x \sum_{m=-1}^{\infty} \left[\frac{\mathrm{d}}{\mathrm{d}x} \left(k' G_{zx} A \left\{ \frac{\mathrm{d}W_m(x)}{\mathrm{d}x} + \Psi_m(x) \right\} \right) W_s(x) a_m(t) - \rho A W_m(x) W_s(x) \ddot{a}_m(t) \right] \mathrm{d}x$$
$$+ f(t) W_s(l_1) = 0. \tag{13}$$

Adding the first eqution to the second in equation (13), we obtain the following relation:

$$\int_x \sum_{m=-1}^{\infty} \left[\left(\frac{\mathrm{d}}{\mathrm{d}x} \left\{ E_x I_z \frac{\mathrm{d}\Psi_m(x)}{\mathrm{d}x} \right\} \Psi_s(x) - k' G_{zx} A \left\{ \frac{\mathrm{d}W_m(x)}{\mathrm{d}x} + \Psi_m(x) \right\} \Psi_s(x) \right.\right.$$
$$\left. + \frac{\mathrm{d}}{\mathrm{d}x} \left(k' G_{zx} A \left\{ \frac{\mathrm{d}W_m(x)}{\mathrm{d}x} + \Psi_m(x) \right\} \right) W_s(x) \right) a_m(t)$$
$$\left. - \{ \rho I_z \Psi_m(x) \Psi_s(x) + \rho A W_m(x) W_s(x) \} \ddot{a}_m(t) \right] \mathrm{d}x + f(t) W_s(l_1) = 0. \tag{14}$$

Each normal mode function in Timoshenko beam theory has the following orthogonal properties:

$$\int_x \{\rho I_z \Psi_m(x)\Psi_s(x) + \rho A\omega_m^2 W_m(x)W_s(x)\}\,\mathrm{d}x = 0 \qquad (m \neq s) \tag{15}$$

$$\int_x \left[\frac{\mathrm{d}}{\mathrm{d}x}\left\{E_x I_z \frac{\mathrm{d}\Psi_m(x)}{\mathrm{d}x}\right\} - k' G_{zx} A\left\{\frac{\mathrm{d}W_m(x)}{\mathrm{d}x} + \Psi_m(x)\right\}\right]\Psi_s(x)$$

$$+ \frac{\mathrm{d}}{\mathrm{d}x}\left[k' G_{zx} A\left\{\frac{\mathrm{d}W_m(x)}{\mathrm{d}x} + \Psi_m(x)\right\}\right] W_s(x)\,\mathrm{d}x = 0 \qquad (m \neq s) \tag{16}$$

$$\int_x \left[\left(\frac{\mathrm{d}}{\mathrm{d}x}\left\{E_x I_z \frac{\mathrm{d}\Psi_m(x)}{\mathrm{d}x}\right\} - k' G_{zx} A\left\{\frac{\mathrm{d}W_m(x)}{\mathrm{d}x} + \Psi_m(x)\right\}\right)\Psi_m(x)\right.$$

$$\left. + \frac{\mathrm{d}}{\mathrm{d}x}\left(k' G_{zx} A\left\{\frac{\mathrm{d}W_m(x)}{\mathrm{d}x} + \Psi_m(x)\right\}\right) W_m(x)\right]\mathrm{d}x$$

$$+ \omega_m^2 \int_x \{\rho I_z \Psi_m(x)^2 + \rho A W_m(x)^2\}\,\mathrm{d}x = 0 \qquad (m = s). \tag{17}$$

When we define the magnitude of the normal mode functions as follows,

$$\int_x \{\rho I_z \Psi_m(x)^2 + \rho A W_m(x)^2\}\,\mathrm{d}x = 1, \tag{18}$$

we obtain a system of uncoupled equations as follows:

$$\ddot{a}_m(t) + \omega_m^2 a_m(t) = W_m(l_1) f(t) \qquad (m = -1, 0, 1, 2, \ldots). \tag{19}$$

Moreover, we need to choose a damping property to treat practical vibrations. In this paper, we define the modal damping ratio ζ_m and assume that the equations of motion in the modal space are expressed as follows:

$$\ddot{a}_m(t) + 2\zeta_m \omega_m \dot{a}_m(t) + \omega_m^2 a_m(t) = W_m(l_1) f(t) \qquad (m = -1, 0, 1, 2, \ldots). \tag{20}$$

As we can calculate the responses of each mode by equation (20), we can obtain the physical responses for flexural displacement w and rotatory displacement ψ by modal superposition in equation (12).

We consider the response at $x = l_x$ when we excite the beam at $x = l_1$ by an impact hammer. Applying the Fourier transform to equation (20) and considering superposition

of each vibration mode, we can obtain the frequency response function, which we call the accelerance, $G(f)$, as follows:

$$\frac{\ddot{W}(l_x, \mathrm{j}\omega)}{F(\mathrm{j}\omega)} = -\sum_{m=-1}^{\infty} \frac{W_m(l_1)W_m(l_x)\omega^2}{\omega_m^2 + 2\mathrm{j}\zeta_m\omega_m\omega - \omega^2}$$

$$= -\sum_{m=-1}^{\infty} \frac{W_m(l_1)W_m(l_x)\omega^2(\omega_m^2 - \omega^2 - 2\mathrm{j}\zeta_m\omega_m\omega)}{(\omega_m^2 - \omega^2 + 2\mathrm{j}\zeta_m\omega_m\omega)(\omega_m^2 - \omega^2 + 2\mathrm{j}\zeta_m\omega_m\omega)}$$

$$= -\sum_{m=-1}^{\infty} \frac{W_m(l_1)W_m(l_x)\omega^2}{(\omega_m^2 - \omega^2)^2 + 4\zeta_m^2\omega_m^2\omega^2}(\omega_m^2 - \omega^2 - 2\mathrm{j}\zeta_m\omega_m\omega) \equiv G(f), \tag{21}$$

where $\omega(=2\pi f)$ denotes the angular frequency in Fourier transform and $\ddot{W}(l_x, \mathrm{j}\omega)$ and $F(l_1, \mathrm{j}\omega)$ are the respective Fourier transforms of the acceleration $\ddot{w}(l_x, t)$ at $x = l_x$ and the input force $f(t)$ at $x = l_1$. Generally, an accelerance depends on input point l_1, output point l_x and frequency f, but we express it as a simplified function of only frequency here. On the other hand, if we could obtain the frequency response, we could regard equation (21) as the function of E_x, G_{zx} and ζ_m $(m = -1, 0, 1, 2, \ldots, M)$.

2.4. OPTIMIZATION METHOD

Now assuming that the dimensions and mass are known, we consider two non-linear optimization problems to obtain model parameters. First, we regard the resonance frequencies in the accelerance as the natural frequencies and we seek values for the elastic constants that will provide best agreement between the natural frequencies obtained by experimental measurements and by the numerical model. We do not include the rigid modes, $m = -1$, 0, since their frequencies are zero and independent of the elastic constants. Now, letting the experimentally obtained natural frequencies be $f_{exp}^{(m)}$ $(m = 1, 2, \ldots, M)$ and those obtained analytically from equation (8) and (11) be $f_{cal}^{(m)}$ $(m = 1, 2, \ldots, M)$, we define the error function $Error(E_x, G_{zx})$ as follows:

$$Error(E_x, G_{zx}) = \frac{1}{M}\sum_{m=1}^{M} \frac{\{f_{exp.}^{(m)} - f_{cal.}^{(m)}\}^2}{\{f_{exp.}^{(m)}\}^2} \tag{22}$$

Second, we formulate identification of model parameters by the accelerance, especially the frequencies and the magnitudes at the resonance points. Calculating equation (21) with the assumption of the values of E_x, G_{zx} and $\zeta_m(m = -1, 0, 1, 2, \ldots)$, we can calculate the frequency response. Therefore we can obtain the frequencies and the magnitudes $(f_{cal.}^{(m)}, G(f_{cal.}^{(m)}))$ at the resonance points. Employing the resonance points $(f_{exp.}^{(m)}, G(f_{exp.}^{(m)}))$ $(m = 1, 2, \ldots, M)$ experimentally obtained, except for the rigid modes, we define the error function $Error(E_x, G_{zx}, \zeta_1, \zeta_2, \ldots, \zeta_M)$ $(m = 1, 2, \ldots, M)$ as follows:

$$Error(E_x, G_{zx}, \zeta_1, \zeta_2, \ldots, \zeta_M) = W_f \sum_{m=1}^{M} \frac{\{f_{exp.}^{(m)} - f_{cal.}^{(m)}\}^2}{\{f_{exp.}^{(m)}\}^2}$$

$$+ W_G \sum_{m=1}^{M} \frac{\{G(f_{exp}^{(m)} - G(f_{cal}^{(m)})\}^2}{\{G(f_{exp}^{(m)})\}^2}, \tag{23}$$

TABLE 2

Mass of materials

Test piece	Dimension (m × m × m)	Mass (kg)
1	$0{\cdot}1 \times 0{\cdot}1 \times 0{\cdot}03t$	$6{\cdot}862 \times 10^{-2}$
2	$0{\cdot}1 \times 0{\cdot}1 \times 0{\cdot}03t$	$6{\cdot}755 \times 10^{-2}$
3	$0{\cdot}1 \times 0{\cdot}1 \times 0{\cdot}03t$	$6{\cdot}750 \times 10^{-2}$
4	$0{\cdot}1 \times 0{\cdot}1 \times 0{\cdot}06t$	$6{\cdot}897 \times 10^{-2}$
5	$0{\cdot}1 \times 0{\cdot}1 \times 0{\cdot}06t$	$7{\cdot}120 \times 10^{-2}$
6	$0{\cdot}1 \times 0{\cdot}1 \times 0{\cdot}06t$	$6{\cdot}863 \times 10^{-2}$

where W_f and W_G are the weights to adjust the difference of orders between the first and the second term on the rightside of equation (23), the relative values of W_f and W_G being chosen to give a reasonable compromise between the fit to the resonance frequencies and that to the magnitudes.

We can now formulate the identification problem as an optimization problem, i.e., identification of elastic constants that minimize the error function (22),

$$\text{Minimize } Error(E_x, G_{zx}) \geqslant 0,$$
$$E_x > 0, \qquad G_{zx} > 0, \tag{24}$$

and that of elastic constants and modal damping ratios that minimize the error function (23)

$$\text{Minimize } Error(E_x, G_{zx}, \zeta_1, \zeta_2, \ldots, \zeta_M) \geqslant 0,$$
$$E_x > 0, \qquad G_{zx} > 0,$$
$$0 \leqslant \zeta_m < 1/\sqrt{2} \qquad (m = 1, 2, \ldots, M), \tag{25}$$

where the fourth constraint for modal damping ratios is necessary for the existence of the resonances. In the calculation of the error function (22), we have to solve the characteristic roots (8) and the frequency equation (11). In the calculation of the error function (23), we also have to use equation (21). These procedures require the solution of the simultaneous non-linear equations and it would be very tedious to express the derivatives of the independent variables explicitly. Therefore, we decide to use a non-linear optimization method not requiring derivatives, the downhill simplex method [14, 15]. Additionally, we apply a penalty function to this method [16] to enforce the required ranges of the parameters.

3. PARAMETER IDENTIFICATION

3.1. AN INERTIAL PARAMETER

When we discuss the dynamic response, the inertia terms play an important role in the motion and we have to determine such parameters as the mass and moment of inertia in rigid body motion. Although the material in this paper has non-uniform structure locally, we assume that we can treat it as a continuum in the dynamic responses and the representative property is a density ρ. In particular, when we consider such flexural models as a plate and a beam, we can define the mass per unit area ρt in plate theory and the mass per unit length ρbt.

We could evaluate the density from the geometry because the sandwich panels in this paper are made from aluminium material and it has regular structure. However, we

TABLE 3

Dimensions of materials

Test piece	Dimensions ($a \times b \times t$)
1	$0{\cdot}8 \times 0{\cdot}1 \times 0{\cdot}03t$
2	$0{\cdot}8 \times 0{\cdot}2 \times 0{\cdot}03t$
3	$0{\cdot}8 \times 0{\cdot}1 \times 0{\cdot}06t$
4	$0{\cdot}8 \times 0{\cdot}2 \times 0{\cdot}06t$

measure the dimensions and the weight for various test pieces experimentally and calculate the density. The dimensions and the corrresponding weights for six 0·1 m × 0·1 m test pieces are shown in Table 2. It is found that all of them have the nearly equal weight regardless of the thickness. Therefore, we take the mass per unit area ρt as the inertia parameter and determine the following value on the average:

$$\rho t = 6{\cdot}880 \text{ kg/m}^2.$$

3.2. EXPERIMENTAL SET-UP

Before identification, we carry out impact testing on four pieces, the dimensions of which are shown in Table 3. A schematic view of the experimental apparatus is shown in Figure 4. To simulate the freely supported boundary conditions, we hang each beam on two lines glued to the beam.

We excite the beam using a small impact hammer and we detect the dynamic response by an accelerometer attached to the beam. The signal is amplified and subjected to a Fast Fourier Transformation (FFT) Analyzer. The data set is transferred to the personal computer through a floppy disk and the required values are obtained. In discrete Fourier transformation, we use the Hanning window as the window function [17].

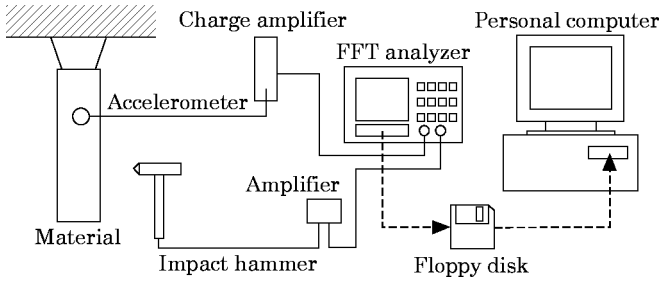

Figure 4. The scheme of the experimental set-up.

TABLE 4

Identified E_x and G_{zx}

	Test piece			
	1	2	3	4
E_x (Pa)	$1{\cdot}070 \times 10^{10}$	$1{\cdot}095 \times 10^{10}$	$4{\cdot}876 \times 10^{9}$	$4{\cdot}849 \times 10^{9}$
G_{zx} (Pa)	$5{\cdot}363 \times 10^{8}$	$5{\cdot}470 \times 10^{8}$	$2{\cdot}980 \times 10^{8}$	$3{\cdot}029 \times 10^{8}$

TABLE 5

Comparison of natural frequencies (*Part* 1) ($a = 0.8$ m, $b = 0.1$ m, $t = 0.03$ m)

Mode no.	Experiment Hz	Calculation Hz
0	0·0	0·0
1	321·3	321·4
2	837·5	837·6
3	1520·0	1522·5
4	2312·5	2306·1
5	3150·0	3141·7
6	3987·5	4000·4

3.3. IDENTIFICATION BY NATURAL FREQUENCIES

At first, we determine the elastic constants E_x and G_{zx} based on the optimization problem of equation (24) so that we can minimize the difference between the experimental and calculated natural frequencies. We adopt six and four elastic modes respectively for the thickness of 0·03 m and 0·06 m in the identification. The obtained elastic constants for the four beams are shown in Table 4. The identified values for the test piece with the same thickness should be equal to each other, since the natural frequencies in the beam model are independent of the width and all test pieces have the same length. As shown in Table 4, the results for the same thickness give nearly equal elastic constants. In Tables 5–8 are shown the comparison of the experimental frequencies with the natural frequencies calculated by equations (8) and (11) with the identified elastic constants. Both sets of results are so identical that these identifications based on Timoshenko theory are valid for test pieces that have the dimensions shown in Table 3.

TABLE 6

Comparison of natural frequencies (*Part* 2) ($a = 0.8$ m, $b = 0.2$ m, $t = 0.03$ m)

Mode no.	Experiment Hz	Calculation Hz
0	0·0	0·0
1	322·5	325·1
2	842·5	847·0
3	1555·0	1539·4
4	2362·0	2331·3
5	3212·5	3175·5
6	3962·5	4043·0

TABLE 7

Comparison of natural frequencies (*Part* 3) ($a = 0.8$ m, $b = 0.1$ m, $t = 0.06$ m)

Mode no.	Experiment Hz	Calculation Hz
0	0·0	0·0
1	582·5	582·9
2	1385·0	1381·8
3	2287·5	2294·2
4	3225·0	3221·0

TABLE 8

Comparison of natural frequencies (Part 4) ($a = 0.8$ m, $b = 0.2$ m, $t = 0.06$ m)

Mode no.	Experiment Hz	Calculation Hz
0	0·0	0·0
1	580·0	582·4
2	1395·0	1383·1
3	2287·5	2300·7
4	3237·5	3234·7

3.4. IDENTIFICATION BY FREQUENCY RESPONSE FUNCTIONS

Secondly, we identify the elastic constants E_x and G_{zx} and the modal damping ratio ζ_m simultaneously by equation (25) as the second optimization problem. Then both the difference in the resonance frequencies and the magnitudes in the experimental and calculated accelerances can be minimized. We adopt six and four resonance points in the accelerances respectively for the thicknesses of 0·03 m and 0·06 m and put the weights W_f as 0·1 and W_G as 10^4 in the evaluation of the function values. When we calculate the accelerance, we put $\zeta_{-1} = \zeta_0 = 0{\cdot}0$. However, as previously mentioned, rigid body motions are not considered in the parameter identification.

The identified elastic constants and modal damping ratios are shown in Table 9. Also in this identification we can obtain similar elastic constants for test pieces with the same thickness, and they are nearly equal to the identified values in the previous section. In Figures 5–8 are shown the comparisons of the experimental accelerances with the accelerances calculated by the identified parameters. As both sets of results agree with each other, we can say that these identifications are valid.

3.5. APPLICATION FOR FEM

Using the identified parameters, we calculate the acceleration time history for impact excitation by FEM and examine the application of identified results for FEM. To reduce error in modelling, we introduce the Timoshenko beam element as a finite element and construct the mass matrix **M** and stiffness matrix **K** [18]. Then we can express the equations of motion for the undamped system as follows:

$$\mathbf{M}\ddot{\mathbf{x}} + \mathbf{K}\mathbf{x} = \mathbf{f}, \tag{26}$$

TABLE 9

Identified E_x, G_{zx} and ζ_m

		Test piece			
		1	2	3	4
E_x (Pa)		$1{\cdot}067 \times 10^{10}$	$1{\cdot}085 \times 10^{10}$	$4{\cdot}954 \times 10^{9}$	$4{\cdot}974 \times 10^{9}$
G_{zx} (Pa)		$5{\cdot}304 \times 10^{8}$	$5{\cdot}390 \times 10^{8}$	$2{\cdot}922 \times 10^{8}$	$3{\cdot}013 \times 10^{8}$
ζ_m	$m = 1$	$2{\cdot}364 \times 10^{-3}$	$1{\cdot}582 \times 10^{-3}$	$2{\cdot}646 \times 10^{-3}$	$4{\cdot}974 \times 10^{-3}$
	$m = 2$	$1{\cdot}306 \times 10^{-3}$	$1{\cdot}271 \times 10^{-3}$	$5{\cdot}509 \times 10^{-5}$	$5{\cdot}465 \times 10^{-4}$
	$m = 3$	$1{\cdot}108 \times 10^{-3}$	$3{\cdot}228 \times 10^{-3}$	$4{\cdot}473 \times 10^{-3}$	$1{\cdot}816 \times 10^{-3}$
	$m = 4$	$2{\cdot}251 \times 10^{-3}$	$2{\cdot}287 \times 10^{-3}$	$5{\cdot}361 \times 10^{-3}$	$8{\cdot}814 \times 10^{-3}$
	$m = 5$	$5{\cdot}485 \times 10^{-3}$	$4{\cdot}403 \times 10^{-3}$	—	—
	$m = 6$	$4{\cdot}488 \times 10^{-3}$	$2{\cdot}510 \times 10^{-3}$	—	—

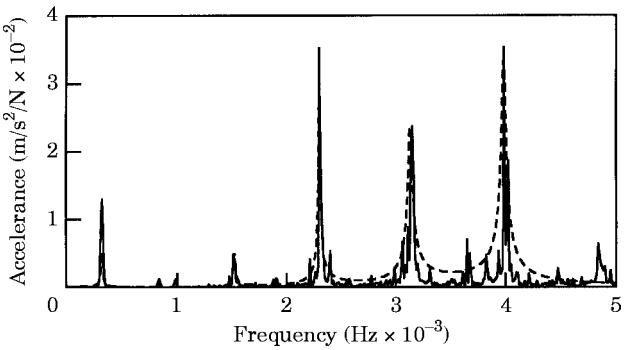

Figure 5. Comparison of the experimental accelerance with the accelerance calculated by the identified parameters: $a = 0{\cdot}8$ m, $b = 0{\cdot}1$ m, $t = 0{\cdot}03$ m. ——, Experiment; – – – –, calculation.

where **x** is the vector of modal displacements and **f** is that of external force. Using the matrix **T** consisting of eigenvectors for this system, we can orthogonalize equation (26) and realize reduction in the modal domain [19]. Namely, putting $\mathbf{x} = \mathbf{T}\mathbf{y}$ and multiplying on the left by $\mathbf{T}^{\mathrm{T}}$, the transpose of **T**, we can reduce the problem in the physical domain to that in the modal domain. Moreover, assuming that we can orthogonalize the damping matrix **C** by the system eigenvector in order to use the identified modal damping ratios,

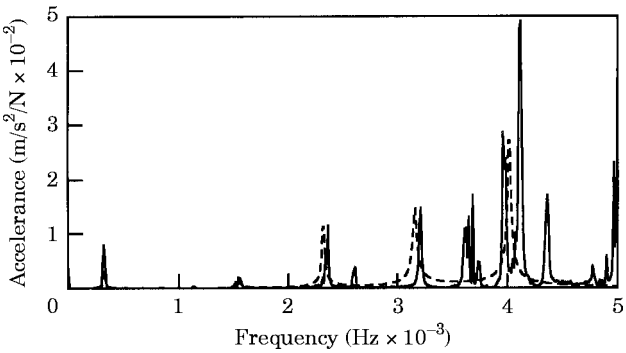

Figure 6. Comparison of the experimental accelerance with the accelerance calculated by the identified parameters: $a = 0{\cdot}8$ m, $b = 0{\cdot}2$ m, $t = 0{\cdot}03$ m. ——, Experiment; – – – –, calculation.

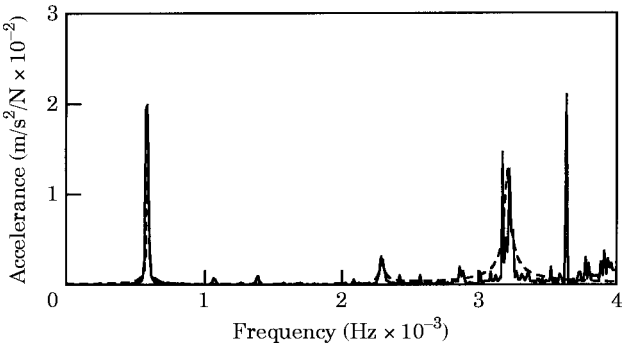

Figure 7. Comparison of the experimental accelerance with the accelerance calculated by the identified parameters: $a = 0{\cdot}8$ m, $b = 0{\cdot}1$ m, $t = 0{\cdot}06$ m. ——, Experiment; – – – –, Calculation.

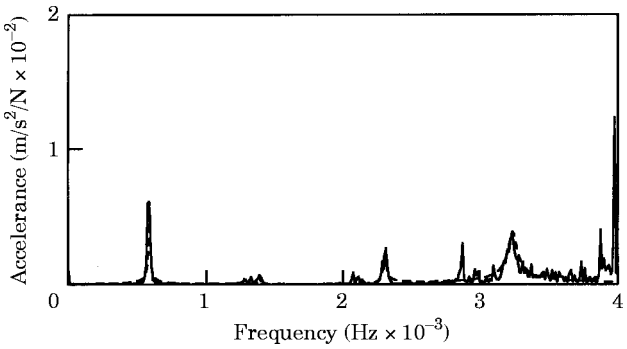

Figure 8. Comparison of the experimental accelerance with the accelerance calculated by the identified parameters: $a = 0{\cdot}8$ m, $b = 0{\cdot}2$ m, $t = 0{\cdot}06$ m. ——, Experiment, – – – –, calculation.

we obtain the damping equations of motion with the modal damping ratios ζ_m in the modal domain as follows:

$$\ddot{\mathbf{y}} + \mathbf{\Lambda}\dot{\mathbf{y}} + \mathbf{\Omega}\mathbf{y} = \mathbf{f}' \tag{27}$$

where $\mathbf{f}' = \mathbf{T}^{\mathrm{T}}\mathbf{f}$,

$$\mathbf{\Omega} = \begin{bmatrix} \omega_{-1}^2 & & & & \mathbf{0} \\ & \omega_0^2 & & & \\ & & \omega_1^2 & & \\ & & & \cdots & \\ \mathbf{0} & & & & \omega_{\mathrm{M}}^2 \end{bmatrix}, \quad \mathbf{\Lambda} = 2 \begin{bmatrix} \zeta_{-1}\omega_{-1} & & & & \mathbf{0} \\ & \zeta_0\omega_0 & & & \\ & & \zeta_1\omega_1 & & \\ & & & \cdots & \\ \mathbf{0} & & & & \zeta_M\omega_M \end{bmatrix}.$$

ω_m ($m = -1, 0, 1, \ldots, M$) denotes the natural angular frequencies obtained by eigenvalue analysis. By the relation of $\mathbf{x} = \mathbf{T}^{-1}\mathbf{y}$, we can tranform the responses in the modal domain

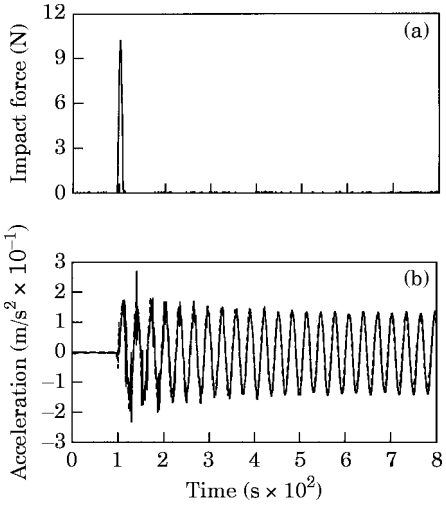

Figure 9. Comparison of the experimental results with those by FEM: $a = 0{\cdot}8$ m, $b = 0{\cdot}1$ m, $t = 0{\cdot}03$ m. ——, Experiment; – – – –, FEM. (a) Time history of impact force; (b) time history of acceleration.

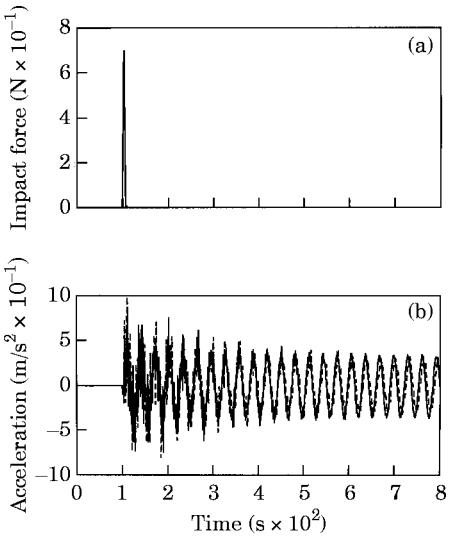

Figure 10. Comparison of the experimental results with those by FEM: $a = 0{\cdot}8$ m, $b = 0{\cdot}2$ m, $t = 0{\cdot}03$ m. ——, Experiment; – – – –, FEM. (a) Time history of impact force; (b) time history of acceleration.

to those in the physical domain and obtain the equations of motion in the physical domain as follows:

$$\mathbf{M}\ddot{\mathbf{x}} + \mathbf{C}\dot{\mathbf{x}} + \mathbf{K}\mathbf{x} = \mathbf{f}. \tag{28}$$

After performing an eigenvalue analysis using the identified elastic constants, the numerical integration of equation (27) is carried out by the Runge–Kutta method. The elastic constants used are the results for the width of 0·1 m, since the material with the narrower width is expected to be closer to the beam model. Namely, we use $E_x = 1{\cdot}067 \times 10^{10}$ P_a and $G_{zx} = 5{\cdot}304 \times 10^8$ Pa for the thickness of $t = 0{\cdot}03$ m and $E_x = 4{\cdot}954 \times 10^9$ P_a and $G_{zx} = 2{\cdot}922 \times 10^8$ Pa for the thickness of $t = 0{\cdot}06$ m. For the damping ratios, we use the

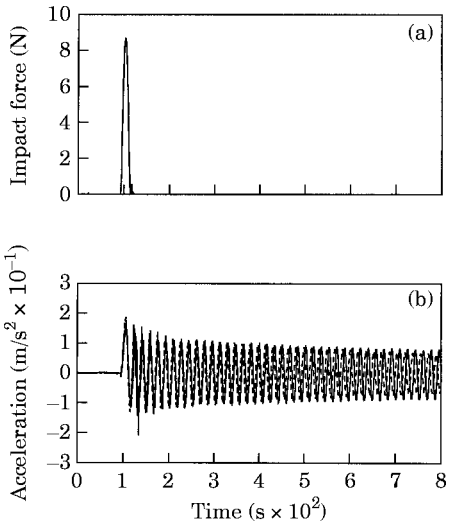

Figure 11. Comparison of the experimental results with those by FEM: $a = 0{\cdot}8$ m, $b = 0{\cdot}1$ m, $t = 0{\cdot}06$ m. ——, Experiment; – – – –, FEM. (a) Time history of impact force; (b) time history of acceleration.

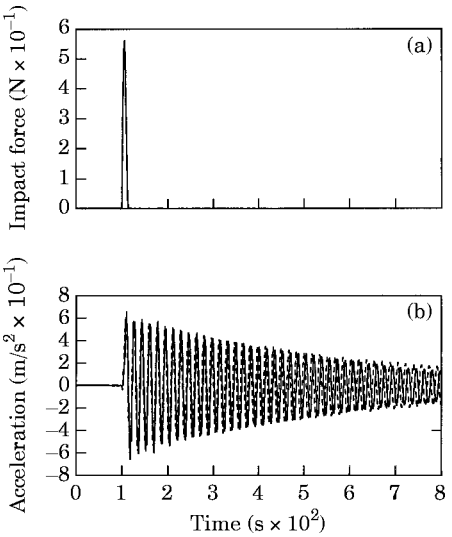

Figure 12. Comparison of the experimental results with those by FEM: $a = 0{\cdot}8$ m, $b = 0{\cdot}2$ m, $t = 0{\cdot}06$ m. ——, Experiment; ——, FEM. (a) Time history of impact force; (b) time history of acceleration.

corresponding experimental values for each case. Moreover, we use the experimental digital data for the input forces directly by the introduction of interpolation. In Figures 9–12 are shown the time histories of the excited impact forces and the resulting accelerations for the four materials shown in Table 3. Solid lines express the experimental results and dotted lines express the calculation results. In all results, the excited point is $x = -0{\cdot}3$ m and the observed point is $x = 0{\cdot}3$ m. The results calculated by FEM agree with the experimental results well. Therefore, the identified values based on this method can be used for FEM analysis.

4. CONCLUSIONS

In the parameter identification of aluminum honeycomb sandwich panels, an orthotropic Timoshenko beam model has been used, and the elastic constants and the modal damping ratios so as to minimize the error between the experimental and analytical results have been determined. The results identified have been applied to FEM. The conclusions can be summarized as follows:

(1) The use of the orthotropic Timoshenko beam is available for the identification of aluminum honeycomb sandwich panels.

(2) Two optimization problems based on the natural frequencies and the accelerances are effective for the parameter identification of aluminum honeycomb sandwich panels. The elastic constants can be easily identified by the experimental and analytical natural frequencies.

(3) The parameters identified by these method can be applied to FEM analysis of the aluminum honeycomb sandwich panels.

REFERENCES

1. J. ZHANG and M. F. ASHBY 1992 *International Journal of Mechanical Sciences* **34**, 475–489. The out-of-plane properties of honeycombs.
2. J. ZHANG and M. F. ASHBY 1992 *International Journal of Mechanical Sciences* **34**, 491–509. Buckling of honeycombs under in-plane biaxial stresses.

3. G. Y. Shi and P. Tong 1994 *American Institute of Aeronautics and Astronautics Journal* **34**, 1520–1524. Local buckling of honeycomb sandwich plates under action of transverse shear forces.
4. G. Y. Shi and P. Tong 1995 *International Journal of Solids and Structures* **32**, 1383–1393. Equivalent transverse shear stiffness of honeycomb cores.
5. M. Grediac 1993 *International Journal of Solids and Structures* **30**, 1777–1788. A finite element study of the transverse shear in honeycomb cores.
6. V. E. Kryutchenko 1995 *Mechanics of Composite Materials* **31**, 352–355. Analysis of the anisotropic properties of honeycomb sandwich plates.
7. R. Butler, A. A. Tyler and W. Cao 1994 *Computers and Structures* **52**, 1107–1118. Optimum design and evaluation of stiffened panels with practical loading.
8. R. D. Adams and M. R. Maheri 1993 *Composites Science and Technology* **47**, 15–23. The dynamic shear properties of structural honeycomb materials.
9. M. R. Maheri and R. D. Adams 1994 *Composites Science and Technology* **52**, 333–347. Steady-state flexural vibration damping of honeycomb sandwich beams.
10. K. Renji, P. S. Nair and S. Narayanan 1996 *Journal of Sound and Vibration* **195**, 687–699. Modal density of composite honeycomb sandwich panels.
11. S. Thwaites and N. H. Clark 1995 *Journal of Sound and Vibration* **187**, 253–269. Nondestructive testing of honeycomb sandwich structures using elastic waves.
12. S. P. Timoshenko, D. H. Young and W. Weaver, Jr. 1974. *Vibration Problem in Engineering*. New York: John Wiley fourth edition.
13. S. P. Timoshenko 1940 *Strength of Materials—Part* 1 170–171. New York: D. Van Nostrand second edition; See pp. 170–171.
14. J. A. Nelder and R. Mead 1964 *Computer Journal* **7**, 308–313. A simplex method for function minimization.
15. J. A. Nelder and R. Mead 1964 *Computer Journal* **8**, 27. A simplex method for function minimization—Errata.
16. R. Fletcher 1981 *Practical Methods of Optimization*, Volume 2, *Constrained Optimization*. New York: John Wiley.
17. The Japan Society of Mechanical Engineers 1995 *Measurement Technic of Vibration and Noise* (in Japanese), Tokyo: Asakura-syoten.
18. T. Yokoyama and K. Kishida 1982 *Technology Report of the Osaka University* **32**, 103–112. Finite element analysis of flexural wave propagation in elastic beams.
19. A. Nagamatsu 1985 *Modal Analysis* (in Japanese). Tokyo: Baifu-kan. See pp. 55–58.